Cdc42 and ARP2/3-independent regulation of filopodia by an integral membrane lipid-phosphatase-related protein

Yury J. Sigal[1], Omar A. Quintero[2,*], Richard E. Cheney[2] and Andrew J. Morris[3,‡]

[1]Department of Cell and Developmental Biology and [2]Department of Molecular and Cellular Physiology, University of North Carolina at Chapel Hill, Chapel Hill, NC 27599-7090, USA
[3]Division of Cardiovascular Medicine and Department of Molecular and Cellular Biochemistry, Gil Heart Institute, University of Kentucky College of Medicine, Lexington, KY 40536-6475, USA

*Present address: Department of Biology, Franklin and Marshall College, Lancaster, PA 17604-3003, USA
‡Author for correspondence (e-mail: a.j.morris@uky.edu)

Accepted 30 October 2006
Journal of Cell Science 120, 340-352 Published by The Company of Biologists 2007
doi:10.1242/jcs.03335

Summary

Filopodia are dynamic cell surface protrusions that are required for proper cellular development and function. We report that the integral membrane protein lipid-phosphatase-related protein 1 (LPR1) localizes to and promotes the formation of actin-rich, dynamic filopodia, both along the cell periphery and the dorsal cell surface. Regulation of filopodia by LPR1 was not mediated by cdc42 or Rif, and is independent of the Arp2/3 complex. We found that LPR1 can induce filopodia formation in the absence of the Ena/Vasp family of proteins, suggesting that these molecules are not essential for the development of the protrusions. Mutagenesis experiments identified residues and regions of LPR1 that are important for the induction of filopodia. RNA interference experiments in an ovarian epithelial cancer cell line demonstrated a role for LPR1 in the maintenance of filopodia-like membrane protrusions. These observations, and our finding that LPR1 is a not an active lipid phosphatase, suggest that LPR1 may be a novel integral membrane protein link between the actin core and the surrounding lipid layer of a nascent filopodium.

Supplementary material available online at
http://jcs.biologists.org/cgi/content/full/120/2/340/DC1

Key words: Filopodia, Actin, cdc42, Lipid phosphatase

Introduction

Actin-rich membrane protrusions are important for many cellular functions, including signaling, neurite outgrowth (Kalil and Dent, 2005), migration and attachment (Perez-Moreno et al., 2003). Regulation of actin organization in cells has been primarily attributed to the functions of small rho family GTPases (Bishop and Hall, 2000; Nobes and Hall, 1995). Cdc42 has been implicated in the regulation of tightly bundled actin filaments that extend from the cell periphery (Etienne-Manneville and Hall, 2002; Nobes and Hall, 1995). These protrusions arise deep within the dendritic actin network, where the growing barbed ends of actin filaments extend and push against the plasma membrane (Wood and Martin, 2002). The filaments are joined together by bundling proteins resulting in straight protrusions, called filopodia (Svitkina et al., 2003). Filopodia vary considerably in length and width, and have distinct patterns of cell surface localization, which probably contribute to their diverse physiological roles (Passey et al., 2004). In the absence of concrete molecular characterization, filopodia are broadly classified as slender membrane protrusions that contain a core of bundled actin filaments (Wood and Martin, 2002). However, in light of recent advances in identification of the mechanisms underlying filopodia formation, classification of these structures can now be based more on the presence of protein machinery responsible for their biogenesis rather than on structural appearance alone.

The best characterized mechanism for the formation of filopodia is termed the ‘convergent elongation’ model which postulates that initiation of filopodia requires activation of the Wiskott-Aldrich syndrome protein (WASP) by cdc42, which in turn recruits and activates the Arp2/3 complex (Svitkina et al., 2003; Welch and Mullins, 2002). Arp2/3 acts as an actin-nucleating complex by binding to the side of an existing actin filament and promoting the growth of a new filament at a 70° angle, thereby generating a branched actin network (Svitkina and Borisy, 1999; Welch and Mullins, 2002). Actin cross-linking proteins such as fascin, can bundle several of these filaments together, which then elongate to form a filopodium (Faix and Rottner, 2006; Svitkina et al., 2003). Capping proteins bind to the tips of actin filaments, thus blocking polymerization and elongation at the barbed ends. Filopodia, however, have Ena/Vasp proteins at their tips (Bear et al., 2000; Bear et al., 2002) which are thought to displace capping proteins and act as ‘leaky caps’, facilitating the addition of actin monomers to elongate the growing filopodia.

Recent evidence, however, has revealed that the convergent elongation model is not universally applicable. Genetic inactivation of cdc42 demonstrated that it is not required for the formation of filopodia in embryonic stem cells (Czuchra et al., 2005). Formation of filopodia was observed in WASP-

deficient cells (Snapper et al., 2001) and depletion of the Arp2/3 complex did not abolish filopodia formation in B16F1 cells (Steffen et al., 2006). More significantly, recent studies have shown that Vasp may not exhibit any anti-capping activity (Samarin et al., 2003), but may rather act as actin-bundling protein required for the formation of filopodia (Schirenbeck et al., 2006). These discrepancies clearly imply that alternative mechanisms for formation of filopodia exist that do not require the Arp2/3 complex, may not depend on cdc42, and probably use anti-capping proteins other then Vasp.

Diaphanous-related formins, such as p134mDia2/Drf3 (mDia2) nucleate actin polymerization independently of Arp2/3 (Evangelista et al., 2003). This large protein exists in a basal autoinhibited conformation, where the N-terminal rho-binding domain (RBD) is associated with the C-terminal diaphanous autoinhibitory domain (DAD), masking the FH2 domain responsible for actin nucleation. When the RBD associates with a small GTPase, the FH2 domain becomes accessible to promote actin polymerization (Evangelista et al., 2003; Peng et al., 2003). Cdc42 has been shown to activate and regulate the activity of mDia2 through interaction with the Cdc42/Rac interactive binding (CRIB) motif of the formin RBD (Peng et al., 2003). mDia2 is also necessary for a novel GTPase called Rho in filopodia (Rif) to induce filopodia in mammalian cell lines independently of cdc42 (Pellegrin and Mellor, 2005). In *Dictyostelium discoideum* the formin dDia2 has also been shown to be necessary for initiation and maintenance of filopodia (Schirenbeck et al., 2005). Although dDia2 is not a complete functional ortholog of mDia2, the two formins share similar characteristics; they are localized to the tips of filopodia where they may serve the dual function of leaky cappers and actin nucleators to promote filopodial growth (Higgs, 2005; Nicholson-Dykstra et al., 2005).

Induction of filopodia clearly requires more than just nucleation of actin polymerization. Actin-bundling proteins such as fascin are required to link parallel actin filaments (Svitkina et al., 2003), and unconventional myosins play a role in transport of proteins along the filopodial core (Sousa and Cheney, 2005). Interactions between these myosins and integrin β-subunits, as well as focal adhesion proteins, may localize these molecules to the shaft and tips of filopodia leading to adhesion of the filopodium to the substratum (Zhang et al., 2004). Formation of filopodia clearly also requires dramatic reorganization of planar regions of the plasma membrane to form a tightly curved membrane 'cylinder' that sheaths the actin core. However, almost nothing is known about the lipid composition of filopodia or, apart from the presence of integrins, about other types of filopodia-localized integral membrane proteins that might play roles in membrane reorganization, or in the localization or tethering of the actin-based machinery responsible for filopodial growth to the inner surface of the plasma membrane. Here we describe a novel integral membrane protein, called lipid-phosphatase-related protein 1 (LPR1), which, when overexpressed in HeLa and Cos7 cells, induces the formation of long and thin filopodia from both the periphery and dorsal surface of the cell. We identify structural determinants in LPR1 that are required for the formation of filopodia. Formation of filopodia by LPR1 is not regulated by cdc42 or Rif and does not require Ena/Vasp family proteins.

Results

Previous work from our laboratory and others identifies a family of integral membrane proteins that we collectively termed LPTs (lipid phosphatases/phosphotransferases) (Sigal et al., 2005). This family consists of five groups of proteins, most of which are enzymes that either dephosphorylate lipid phosphates, or catalyze transphosphatidylation reactions involved in the metabolic interconversion of phosphatidylcholine and sphingomyelin. One of the less well-studied groups of the LPT family contains four genes, which we provisionally termed lipid-phosphatase-related (LPR) proteins. Like all LPT family members, these proteins contain a core domain with six

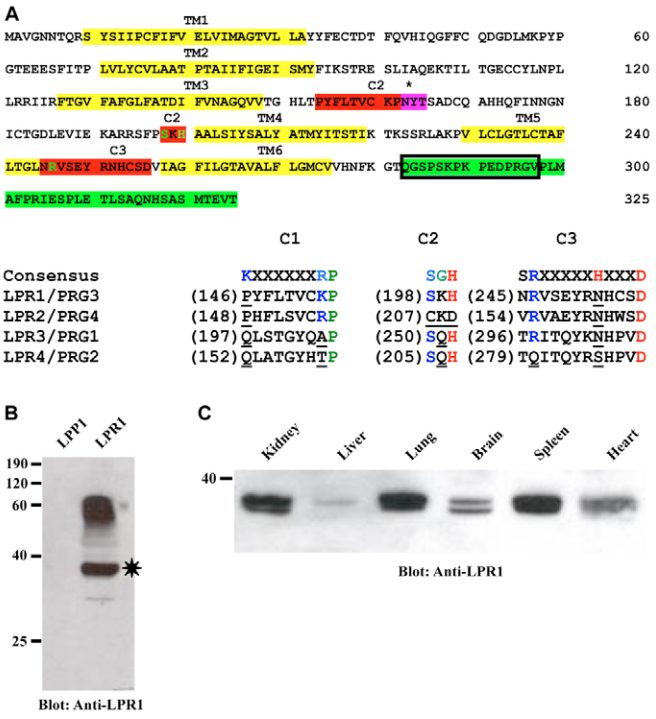

Fig. 1. LPR1 is a widely expressed integral membrane protein with a variant lipid phosphate phosphatase catalytic motif. (A) The deduced amino acid sequence of human LPR1 with hydrophobic residues that are predicted to form six transmembrane α-helices highlighted in yellow. Residues corresponding to the consensus phosphatase motif found on the LPPs and other family members are highlighted in red. The site of glycosylation is highlighted in purple and the sequence used to generate the LPR1 antibody is boxed. Residues shown in green font were mutated as described in the text. The C-terminus highlighted in green corresponds to the last 43 residues deleted to form the LPR1 C-term Δ43 mutant described in the text. The consensus phosphatase sequence motif is shown below in alignment with cognate sequences from four proteins of the LPR family. Residues that participate in the charge relay catalytic mechanism of the phosphatase reaction are highlighted in red and residues that contact the substrate or transition state phosphate group are highlighted in blue. Residues within this motif that are divergent in LPR1 and related proteins are underlined. (B) Membrane protein preparations from insect cells expressing LPP1 or LPR1 were analyzed by western blotting using an LPR1-specific antibody. Asterisk denotes an LPR1-specific immunoreactive band of 35-38 kDa. Samples contained equal quantities of proteins. (C) LPR1 expression in mouse tissues was analyzed by western blotting. Samples contained equal quantities of protein.

predicted transmembrane helices linked by intra- and extramembrane loops. The third of these contains a consensus glycosylation sequence. The active site of the LPT family enzymes is formed from residues within the third and fifth extramembrane loops (Fig. 1A). However, comparison of the relevant regions of the LPR proteins with those of other members of the LPT family reveals that a number of crucial catalytic residues are missing. (Fig. 1A) (see also Sigal et al., 2005). This observation implies that LPR proteins could not catalyze lipid phosphatase or phosphotransferase reactions using the mechanism defined for other LPT family enzymes. To explore this issue directly, LPR1 was expressed in insect cells using a baculovirus vector. This system is highly effective for expression and characterization of another group of LPT proteins, the lipid phosphatase phosphatases (LPPs). Because endogenous levels of LPP activity are low in these cells, strong overexpression obtained using baculovirus vectors allows the use of membranes or detergent membrane extracts from LPP-expressing cells as a source of protein for measurements of enzyme activity (Roberts et al., 1998). Recombinant LPR1 was detected as a strongly immunoreactive species of the expected molecular mass using an antibody raised against an LPR1-specific peptide sequence that is conserved between the murine and human forms of the protein (Fig. 1B). The higher molecular mass species probably represents an aggregated form of this hydrophobic protein. LPPs1-3 exhibit characteristically broad specificity for a range of lipid phosphate substrates and are highly active against substrates presented in mixed micelles with non-ionic detergents (Brindley and Waggoner, 1998). Hydrolysis of four well characterized LPP substrates, lysophosphatidic acid (LPA), phosphatidic acid (PA), sphingosine 1-phosphate (S1P) and ceramide 1-phosphate (C1P) was measured by detergent extracts from Sf9 cells infected with a control virus or with viruses for expression of LPP1 or LPR1. Whereas dramatic (~250-fold) increases in activity against each of these substrates were observed in extracts from cells expressing LPP1, there was no significant increase in phosphatase activity against any of these substrates in extracts from LPR1-expressing cells (Table 1). LPPs1-3 can also hydrolyze substrates in complex with BSA, but again no increases in hydrolysis were observed when these substrates were incubated with extracts from cells expressing LPR1. These observations are consistent with our previous finding that mammalian cells expressing LPR1 or LPR3, or membrane fractions derived from these cells, do not exhibit increased LPA phosphatase activity (McDermott et al., 2004).

RNA analysis suggests that LPR1 is a widely expressed protein (Sigal et al., 2005). To explore this directly, expression of LPR1 in different mouse tissues was examined by western blotting. LPR1 was detected as a doublet of immunoreactive protein with molecular mass of ~35-38 kDa in all tissues examined (Fig. 1C). As noted above, LPR1 contains a consensus glycosylation site within the third extramembrane loop. Studies using epitope-tagged recombinant LPR1 identify N165 as the site of glycosylation, and we observed that the LPR1 species of lower mobility on SDS-PAGE could be converted to the more mobile species by treatment with N-glycosidase (our unpublished observations). These results indicate that the immunoreactive LPR1 species detected in mouse tissues probably represent immature and mature glycosylated forms of the protein.

Table 1. LPR1 does not hydrolyze phospholipid substrates under conditions that readily support LPP1 activity

	Phosphatase activity (pmol/minute/mg)			
	Substrates (mixed micelles)			
	LPA	PA	C1P	S1P
Control	0.11±0.03	0.13±0.02	0.10±0.01	0.14±0.03
LPP1	32±0.1	45±2.6	27±3.0	26±1.1
LPR1	0.10±0.03	0.14±0.04	0.14±0.05	0.16±0.05
	Substrates (BSA)			
	LPA	PA	C1P	S1P
Control	0.02±0.002	0.02±0.002	ND	0.07±0.009
LPP1	2.3±0.2	3.1±0.1	ND	2.1±0.1
LPR1	0.02±0.003	0.03±0.001	ND	0.04±0.002

LPP1 and LPR1 were expressed in insect cells using baculovirus vectors and initial rates of substrate hydrolysis determined using purified membranes or detergent extracted membrane proteins as a source of activity using the indicated substrates and the procedures described in the text. ND, not determined. The data show mean ± s.d. from triplicate determinations and are representative of three experiments.

EGFP-LPR1 labels dynamic, actin-rich membrane protrusions identified as filopodia

LPR1, also termed PRG3, has been previously reported to induce formation of 'neurites' when expressed in cultured N1E-115 and Cos7 cells, although no characterization of these structures was performed (Savaskan et al., 2004). LPR1 was expressed in HeLa and Cos7 cells by transient transfection. The recombinant protein incorporated a C-terminal EGFP tag. Western blot analyses of extracts from these cells revealed that the EGPF-LPR1 protein was strongly expressed at the predicted molecular mass (Fig. 2E and data not shown) (see also McDermott et al., 2004). Indirect immunofluorescence analysis of fixed cells revealed that the protein was localized to both intracellular membrane structures (probably the endoplasmic reticulum and Golgi complex) and to the plasma membrane. Distribution of LPR1 along the plasma membrane appeared discontinuous, with a pronounced localization to many thin membrane protrusions up to ~5 μM in length. LPR1 was predominantly distributed uniformly along the shafts of these protrusions, with an occasional enrichment at their tips (Fig. 2B,D). We do not know the extent to which this apparent enrichment of LPR1 to these protrusions results from their increased membrane density in comparision with other regions of the plasma membrane. Analysis of cells expressing LPR1 by wide-field and confocal fluorescence microscopy showed that these protrusions were rich in polymerized actin and were distributed around both the periphery and across the dorsal surface of the cell (Fig. 2B,D,F). These types of membrane protrusions were not labeled when EGFP-tagged LPP3 (an enzymatically active LPP that also localizes to the plasma membrane and intracellular membranes) or EGFP alone were expressed in these cells (Fig. 2A). Because GFP can self-associate (Yang et al., 1996), we were concerned that the dramatic morphological phenotype induced by expression of EGFP-LPR1 might be artifactually produced by clustering of the GFP tags, resulting in an accumulation of the overexpressed integral membrane protein, which could in turn distort the plasma membrane. To address this issue, LPR1 containing a C-terminal HA epitope tag was expressed in Cos7

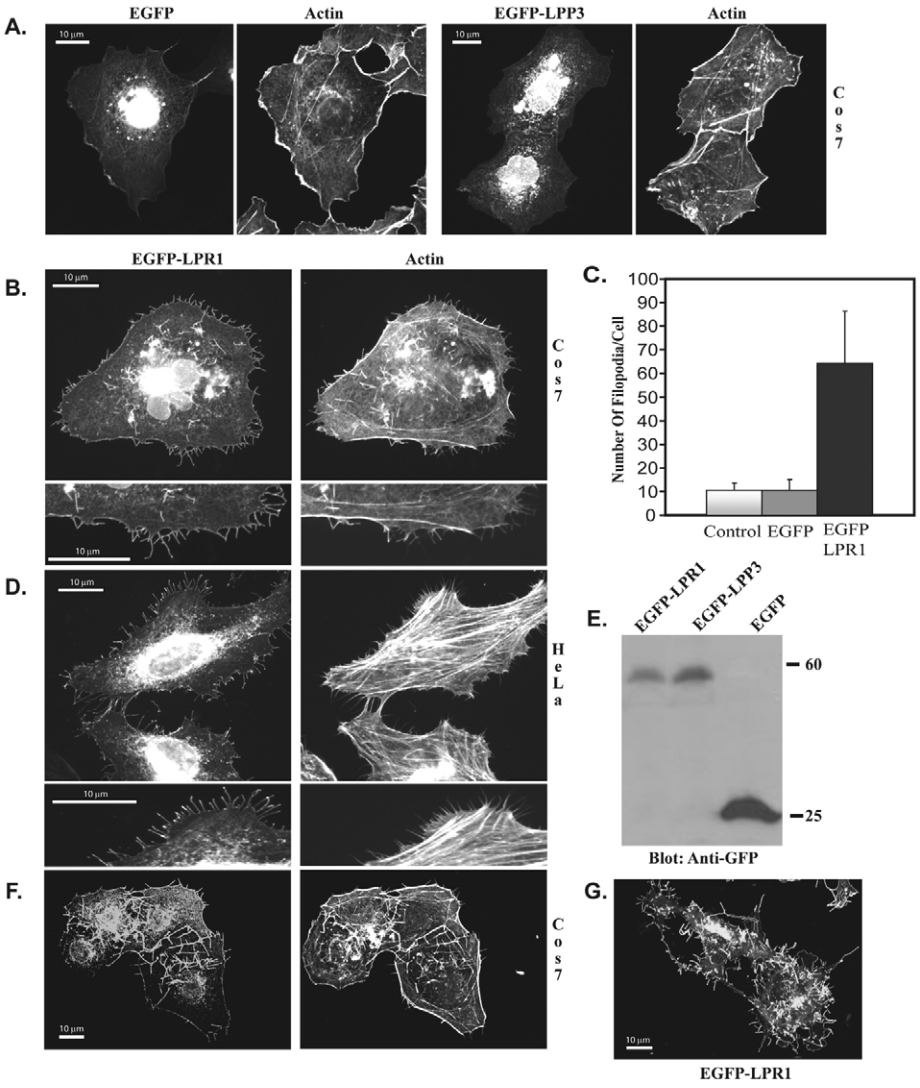

Fig. 2. LPR1 localizes to and increases the number of actin-rich membrane protrusions in HeLa and Cos7 cells. Cos7 cells were transfected with pEGFP, pEGFP-LPP3 (A) and pEGFP-LPR1 (B) and the distribution of EGFP-tagged protein and actin organization were visualized by immunofluorescence microscopy. (C) Bar graph comparing the number of filopodia, dorsal and peripheral, as visualized by phalloidin staining, in untransfected (control) Cos7 cells and Cos7 cells expressing either EGFP or EGFP-LPR1. Twenty cells were counted for each category; error bars denote s.d. for each group. (D). HeLa cells were transfected with pEGFP-LPR1 and localization of the protein and actin organization were determined by fluorescence microscopy. All images were acquired and processed identically. Panels B and D contain higher magnification images of sections of the cell periphery in the images above to show actin staining and LPR1 localization to filamentous structures. (E) Cell lysates from HeLa cells transfected with pEGFP, pEGFP-LPP3 or pEGFP-LPR1 were examined by western blotting with a GFP-specific antibody. Each lane was loaded with equal amounts of total protein. (F) Cos7 cells were transfected with pEGFP-LPR1, fixed, counterstained with Rhodamine phalloidin, and analyzed by confocal microscopy. Images are shown as projections of *z* sections in both Rhodamine and GFP channels. (G) Cos7 cells were transfected with pEGFP-LPR1, and examined live by confocal microscopy. The image represents a projection of *z* sections at a single time interval in a GFP-specific channel. Bars, 10 μm.

and HeLa cells which were examined by indirect immunofluorescent microscopy. Overexpression of Ha-LPR1 resulted in the labeling of multiple actin-rich filopodia that were identical to filopodia observed upon transient expression of EGFP-LPR1 (supplementary material Fig. S1A,B compare with Fig. 2B,D).

Because of concerns about preserving fragile membrane protrusions in fixed specimens, we also examined EGFP-LPR1 expressing live Cos7 cells by confocal microscopy. Again, we observed labeling of many membrane protrusions, both at the cell periphery and across the dorsal surface (Fig. 2G). We used video microscopy to analyze the dynamics of the structures labeled with LPR1 in live cells. Dynamic protrusions, such as filopodia, should exhibit both retractile and protrusive behavior, independent of the movement of the cell (Atilgan et al., 2006). These could be distinguished by time-lapse microscopy from retraction fibers, which are formed by membrane remnants that remain anchored as motile cells move across the substratum. Fig. 3A,B shows a time-resolved series of phase and EGFP fluorescence images of a section of two different HeLa cells expressing EGFP-LPR1. Panels in Fig. 3A showed that in a time period of 6 minutes, the majority of LPR1-labeled protrusions were retracting relative to the motionless cell. Images in Fig. 3B illustrated that LPR1-labeled projections were extending throughout a period of three minutes, with a few nascent LPR1-labeled protrusions forming from the periphery of the stationary cell. The videos, from which the data shown in Fig. 3A is derived, are presented as supplementary material Movies 1 and 2, while images from Fig. 3B are acquired from supplementary material Movies 3 and 4. Taken together, the highly dynamic nature of the filamentous plasma membrane protrusions observed in cells expressing LPR1, their morphology and actin composition, identifies them as filopodia.

Overexpression of LPR1 increases the number of filopodia in different cell types

To ascertain whether overexpressed LPR1 localizes to and labels preexisting filopodia, or itself induces the formation and labeling of new filopodia, we quantified actin-rich phalloidin-stained plasma membrane protrusions in both HeLa and Cos7 cells expressing EGFP-LPR1 and compared this to cells expressing EGFP alone. HeLa cells have a strongly defined actin cytoskeleton, which, when labeled with phalloidin to

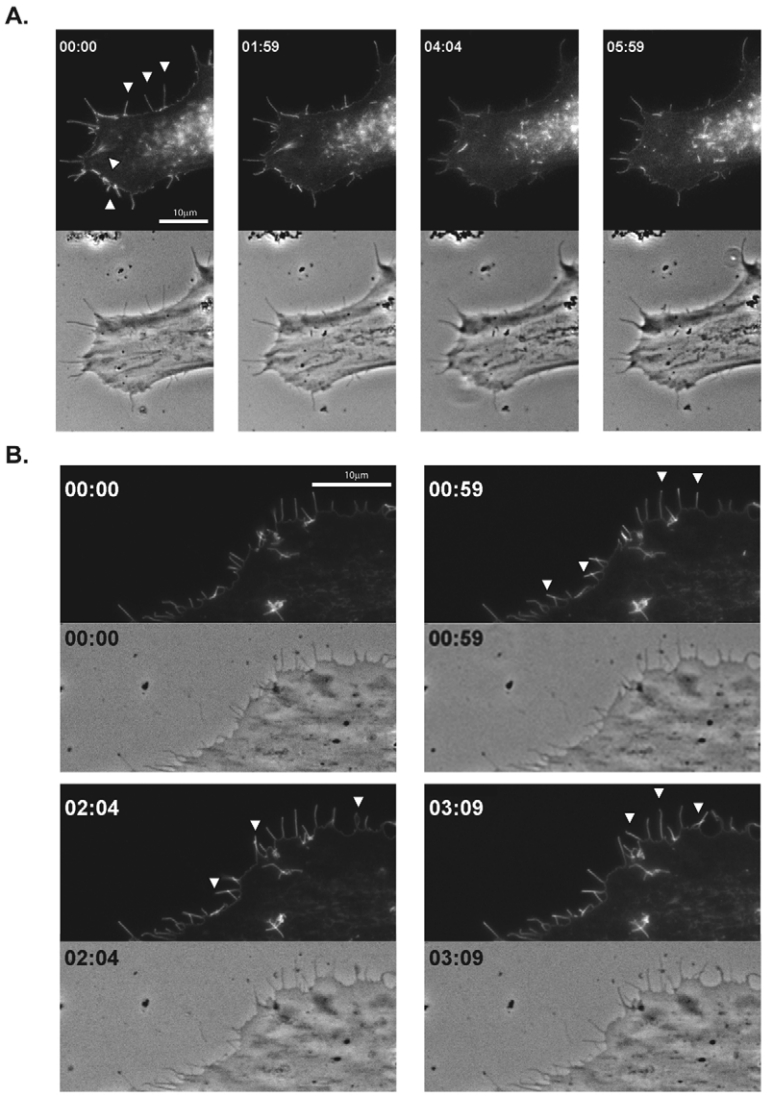

Fig. 3. LPR1-labeled filopodia are dynamic and exhibit both retractile and protrusive motion. Phase-contrast (lower frame) or EGFP fluorescence (upper frames) images of two HeLa cells expressing EGFP-tagged LPR1 are shown. The panels are individual frames taken from supplemental material Movies 1-4. The numbers on each panel denote the time at which each image was captured. (A) Arrows denote filopodia that steadily diminished in length throughout the period observed. (B) Arrows in each panel indicate either newly formed filopodia or filopodia that have increased in length compared with the previous time frame. Bars, 10 μm.

visualize actin, masks actin-rich dorsal protrusions because of the presence of numerous cytoplasmic actin stress fibers. For this reason, quantification of filopodia in HeLa cells was limited to counting peripheral filopodia. Despite this limitation, an approximate doubling in the number of these protrusions was observed in these cells (data not shown). Cos7 cells are more uniform in size than HeLa cells, and have fewer stress fibers, making it easier to visualize and count dorsal filopodia, allowing for a more precise estimate of the effects of LPR1 expression on the number of filopodia displayed by these cells. We therefore quantified both dorsal and peripheral filopodia in Cos7 cells expressing EGFP-LPR1 and compared this number with the number of filopodia in cells expressing EGFP alone. The results (Fig. 2C) illustrate that there is an approximately sixfold increase in the number of filopodia in Cos7 cells expressing EGFP-LPR1 (64.4 filopodia per cell) versus untransfected (control) or EGFP-expressing cells, which both exhibit a mean number of 10.5 filopodia per cell. Overexpression of LPR1, therefore, results in an approximate doubling in the number of peripheral filopodia in HeLa cells and an approximately sixfold increase in the total number of filopodia in COS7 cells, the majority of which are on the dorsal surface. In both cell types, all filopodia detected by actin staining also contained LPR1 suggesting that, in addition to inducing and labeling new filpodia, LPR1 also localizes to filpodia that are formed spontaneously by these cells.

Identification of residues and regions of LPR1 that are important for the induction of filopodia

LPR1 contains a variant LPT catalytic motif in which amino acid residues crucial for catalysis are not conserved. Attempts to 'restore' catalytic activity of LPR1 by reconstituting the active site using site-directed mutagenesis were not successful (data not shown). However, in the course of these studies, we identified a possible role for residues within the 'catalytic core' of the protein in the induction of filopodia. LPR1 variants containing non-conservative substitutions of Ser198 and His200 within the C2 motif and Arg246 from the C3 motif (Fig. 1A) were found to be strongly expressed in transient transfection experiments but failed to induce the formation of filopodia in HeLa cells (supplementary material Fig. S2A,D). In contrast to wild-type LPR1, these mutant LPR1 proteins were, within the detection limits of our experiments, exclusively localized to intracellular membranes. These residues are predicted to be involved in substrate recognition by active members of the LPT family, and substitution of these residues in members of the LPP family produces inactive enzymes (Sigal et al., 2005; Starz-Gaiano et al., 2001). Although LPR1 is enzymatically inactive, association of LPR1 with as yet unidentified lipids may therefore be important for trafficking of the protein to the plasma membrane and in the induction of filopodia.

Alignment of all four LPR family members revealed that a short sequence within the C-terminus proximal to the final transmembrane domain is highly conserved within this family of proteins. A variant of LPR1 in which the C-terminal 43 residues was deleted (EGFP-LPR1 C-term Δ43) exhibited a significantly attenuated ability to induce the formation of peripheral filopodia in HeLa cells compared with wild-type LPR1, despite being expressed at a comparable level (supplementary material Fig. S2B,C). In contrast to the point mutants described above, subcellular distribution of EGFP-LPR1 C-term Δ43 between the plasma membrane and intracellular membranes was highly comparable with that of wild-type LPR1. Since the number of peripheral filopodia observed in cells expressing EGFP-LPR1 C-term Δ43 was equivalent to the number of peripheral filopodia observed in control cells, as determined by phalloidin staining

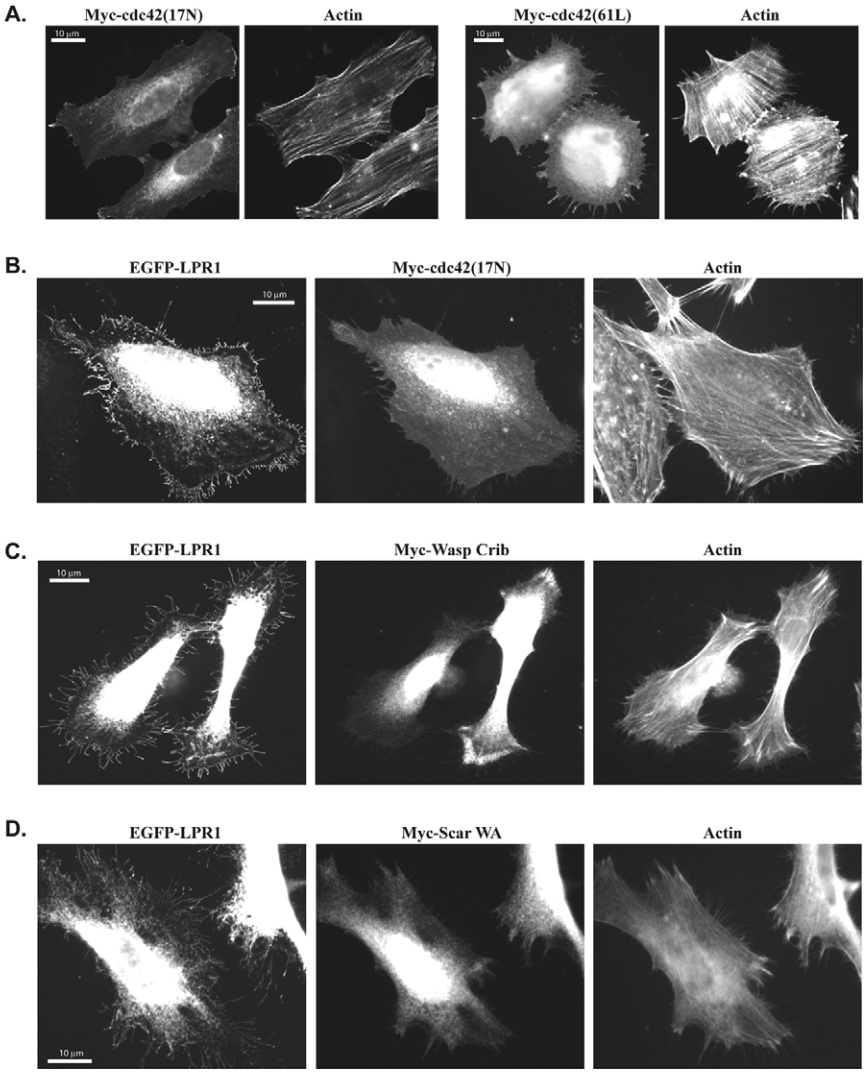

Fig. 4. Effects of LPR1 on filopodia are not mediated by the small GTPase cdc42. (A) HeLa cells were transfected with vectors for expression of myc-tagged cdc42Q 61L or cdc42T 17N. HeLa cells were transfected with vectors for expression of EGFP-LPR1 and myc-tagged constructs of cdc42T 17N (B), Wasp-CRIB (C) and Scar-WA (D). In all cases, EGFP- and myc-tagged proteins and actin organization were visualized by fluorescence microscopy. Bars, 10 μm.

(supplementary material Fig. S2C), we propose that LPR1 C-term Δ43 mutant is incapable of generating new filopodia, but rather localizes to pre-existing endogenous protrusions extended by these cells. These results identify a crucial role for the C-terminal 43 amino acids of LPR1 in the induction of filopodia.

Induction of filopodia by overexpression of LPR1 is independent of the small GTPase cdc42 and its effectors

Overexpression of activated alleles of several small GTPases, most prominently cdc42, induces the formation of membrane protrusions in many cell types (Etienne-Manneville and Hall, 2002). HeLa cells expressing constitutively active cdc42 Q61L extended membrane protrusions that were noticeably thicker and shorter than membrane extensions labeled by expression of EGFP-LPR1 (Fig. 4A, compare with Fig. 2D). Furthermore, HeLa cells expressing constitutively active cdc42 were noticeably smaller and rounder then both wild-type cells, and cells expressing EGFP-LPR1. Induction and labeling of filopodia in EGFP-LPR1-expressing cells was apparent 12-24 hours after transfection and maintained for up to 48 hours, whereas extension of filopodia observed in cells expressing cdc42 Q61L was markedly more transient. Expression of the dominant-negative-acting cdc42 mutant, cdc42 17N, had no obvious effects on cell morphology (Fig. 4A). Formation of filopodia by EGFP-LPR1 was not attenuated by co-expression with Cdc42 T17N in HeLa cells (Fig. 4B, Fig. 5C) or Cos7 cells (data not shown), suggesting that the effect of LPR1 on formation of filopodia is not mediated by cdc42.

To further explore the possible involvement of cdc42 and its effector, the ARP2/3 complex, in the formation of filopodia in LPR1-expressing cells, we used strategies recently used in the study of another small GTPase, Rif, as a novel regulator of filopodia (Pellegrin and Mellor, 2005). EGFP-LPR1 was co-expressed with a WASP CRIB motif, which has been shown to sequester and thereby inhibit the function of cdc42 (Nobes and Hall, 1999; Pellegrin and Mellor, 2005). Co-expression with this construct had no effect on the ability of LPR1 to induce filopodia in HeLa cells (Fig. 4C). EGFP-LPR1 was also co-expressed with the SCAR WA domain that has been reported to sequester and thereby inhibit the function of ARP2/3 (Machesky and Insall, 1998; Pellegrin and Mellor, 2005). Again, there was no decrease in the number of filopodia in cells expressing the two constructs (Fig. 4D); however, the overall morphology of the cells was slightly affected by expression of this protein fragment.

LPR1-induced filopodia resemble filopodia produced by expression of Rif, but are not attenuated in the presence of dominant negative Rif construct

HeLa cells expressing either wild-type (Rif WT) or constitutively active Rif (Rif Q75L) extend numerous filopodia from both the dorsal and peripheral surfaces (Pellegrin and Mellor, 2005) (Fig. 5A). These protrusions closely resemble filopodia induced and labeled by LPR1 in length and thickness and cellular orientation. Co-expression of a dominant-negative-acting mutant of Rif, Rif33TN, with EGFP-LPR1 in HeLa cells did not abolish or diminish filopodia extended by these cells (Fig. 5B,C). These results suggest that LPR1 does not function upstream of Rif in the regulation of filopodial organization but does not exclude the

possibility that LPR1 and Rif operate through a common effector pathway.

LPR1-labeled filopodia have a unique protein composition

In some cell types, the tips of cdc42-regulated filopodia contain focal adhesion proteins, such as paxillin and vinculin (Nobes and Hall, 1995). HeLa cells transiently expressing EGFP-LPR1 lack paxillin at the tips of LPR1-labeled filopodia (Fig. 6A). These focal adhesion markers were predominantly localized to the base of LPR1-based filopodia, most prominently between adjacent protrusions. Vasp, another component of focal adhesions (Bear et al., 2000; Holt et al., 1998), is also a putative anti-capping protein that is localized to the tip complex of cdc42-induced filopodia (Krugmann et al., 2001; Welch and Mullins, 2002). By contrast, we observed that although Vasp was clearly detected at the tips of cdc42-mediated filopodia (supplementary material Fig. S3), within the detection limits of our experiments, it was excluded from the tips and shafts of LPR1-labeled filopodia (Fig. 6B). As observed with another focal adhesion protein, paxillin, VASP was localized to the base of LPR1-labeled filopodia, where it might function in maintaining cellular attachment to the substratum. Two VASP homologs, Mena and Evl, exhibited identical localization patterns (data not shown).

We examined the localization of several additional proteins to filopodia induced by overexpression of activated LPR1. Myosin X, localizes to the tips of cdc42 mediated filopodia, where it may function in the transport of proteins to the filopodial tips (Sousa and Cheney, 2005; Tokuo and Ikebe, 2004). Our results (Fig. 6C) indicated that myosin-X also clearly localizes to the tips of filopodia in HeLa cells expressing LPR1. Actin bundling proteins, such as fascin are crucial proteins for the formation of filopodia and filopodia-like structures in vivo and in vitro (Svitkina and Borisy, 1999; Vignjevic et al., 2003). In fact fascin is considered to be a definitive marker for filopodia. Indirect immunofluorescence analysis using the fascin-specific antibody used in this study requires treatment of cells with methanol, followed by paraformaldehyde fixation, which sometimes results in a loss of fine structures such as filopodia. Fascin uniformly decorated the shafts of LPR1 labeled filopodia in Cos7 cells, suggesting that formation of filopodia by LPR1 is likely to require the actin-bundling activity of this protein. Similar results were seen in HeLa cells, although filopodia in this cell line were not well preserved following treatment with methanol (data not shown).

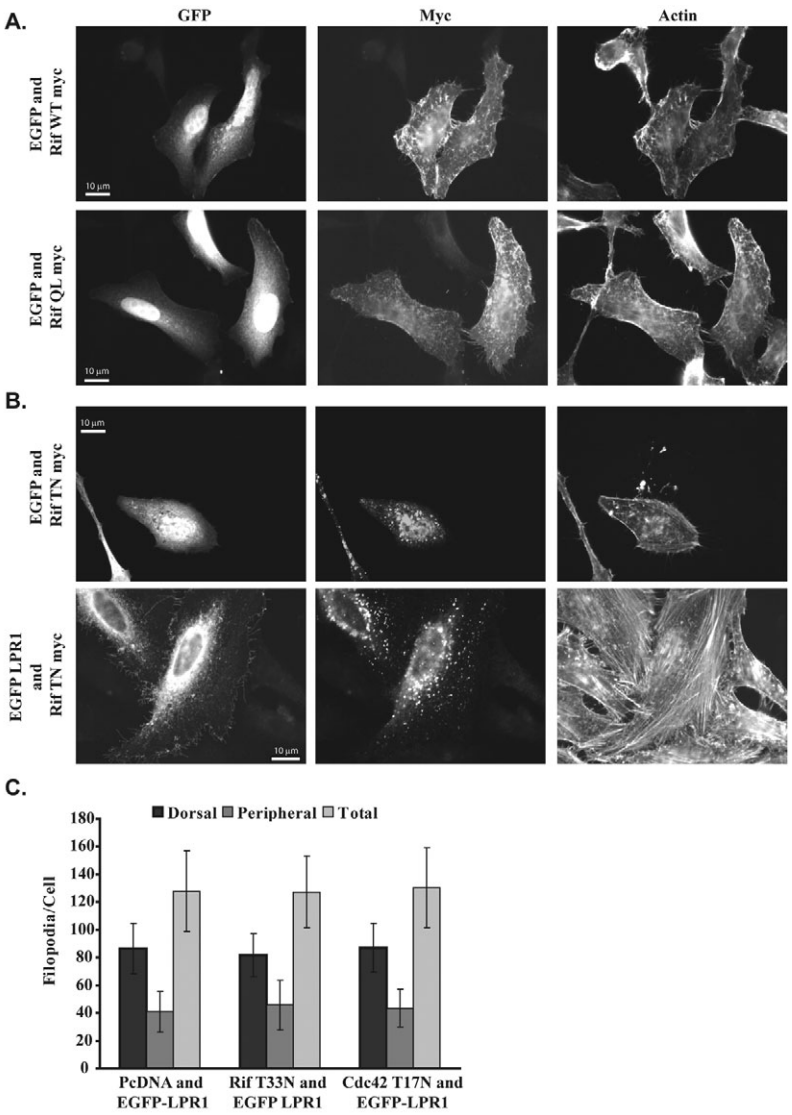

Fig. 5. LPR1-induced filopodia resemble filopodia produced by expression of Rif, but LPR1-induced filopodia are not attenuated by co-expression with a dominant-negative-acting Rif mutant. (A) HeLa cells were co-transfected with plasmids expressing EGFP and either myc-tagged wild-type Rif (Rif WT myc), or myc-tagged constitutively active Rif (Rif QL myc). (B) HeLa cells were co-transfected with vectors encoding for myc-tagged dominant-negative Rif (Rif TN myc) and either EGFP alone or EGFP-tagged LPR1 (EGFP-LPR1). EGFP- and myc-tagged proteins, as well as actin, were examined by fluorescent microscopy in A and B. Bars, 10 μm. (C) HeLa cells were transfected with EGFP-LPR1 and either pcDNA, Rif TN myc or myc-Cdc42 (17N). EGFP-LPR1-labeled dorsal and peripheral filopodia were counted in 25 individual cells. The data shown are means ± s.d.

LPR1 induces filopodia in the absence of Ena/Vasp proteins

Given that, within the detection limits of the immunofluorescence approach, we were not able to detect any endogenous Vasp at the tips of LPR1-induced filopodia, a concern was raised that the slender nature of these protrusions limited our ability to detect any visible amounts of these proteins at the tips of these structures. To fully dissect the role of Vasp in LPR1-mediated filopodial protrusion we expressed EGFP-LPR1 in MV^{D7} cells. These cells have been engineered to lack any of the three members of the Vasp family (Bear et al., 2000). Scanning electron microscopy of these cells has

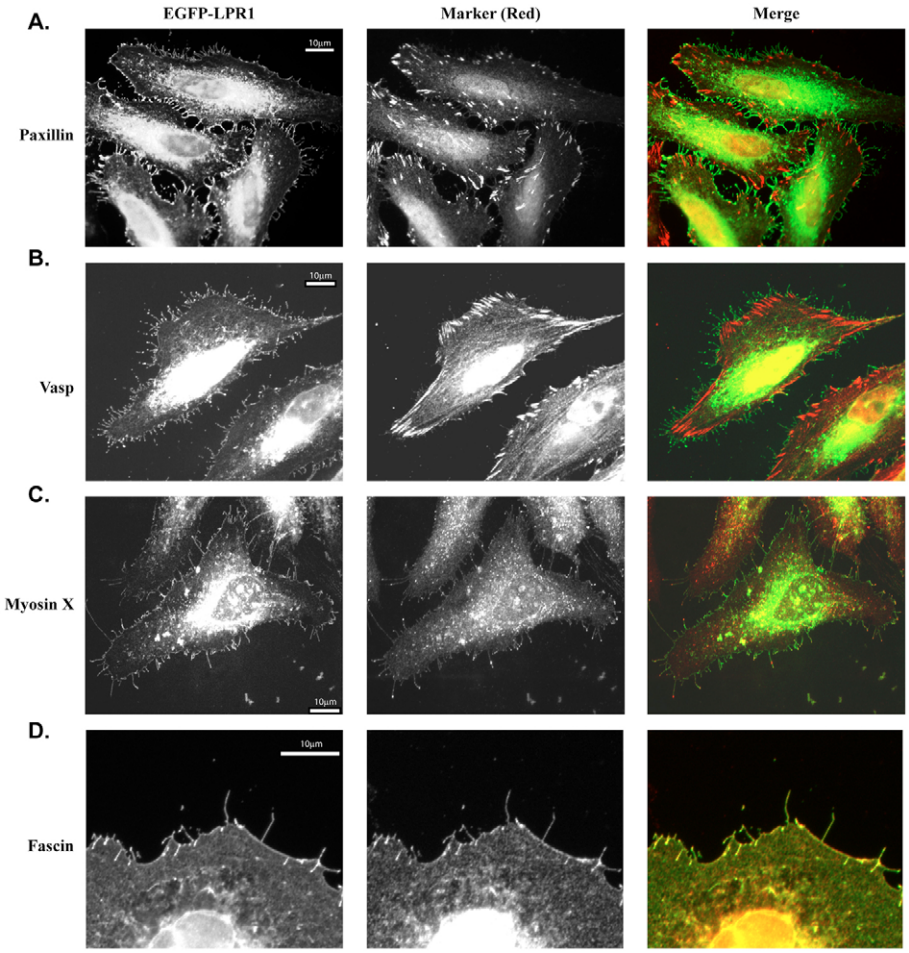

Fig. 6. LPR1-labeled filopodia have a unique protein composition. HeLa cells were transfected with pEGFP-LPR1, and immunofluorescence microscopy was used to visualize EGFP-tagged LPR1 and different endogenously expressed proteins: paxillin (A), Vasp (B) and myosin X (C). (D) Cos7 cells were transfected with vectors for expression of EGFP-LPR1 and localization of endogenous fascin and EGFP-LPR1 were analyzed by immunofluorescence microscopy. Fascin labels intracellular structures as well as membrane protrusions. High magnification images of the periphery of the cells show how these markers localize exclusively within the filopodia. Bars, 10 μm.

shown that they lack any endogenous dorsal filopodia, and have very few endogenous peripheral protrusions (Bohil et al., 2006). MV^{D7} cells expressing EGFP-LPR1 extend numerous filopodia from the periphery and especially the dorsal surface of the cell. These are clearly labeled with actin (Fig. 7A) and fascin (Fig. 7B) suggesting that these structures are true filopodia. This result definitively demonstrates that LPR1 can generate filopodia in the absence of Vasp, or its functional homologs.

LPR1 is required for maintenance of membrane protrusions in ovarian epithelial cancer cells

Because overexpression of LPR1 increased the number of filopodia in HeLa, Cos7 and MV^{D7} cells we sought to investigate the normal role of this protein in the formation and maintenance of these structures. RNA analysis and immunohistochemistry indicate that LPR1 expression is high in epithelial tissues and cell lines (Sigal et al., 2005) (our unpublished observations). SK-OV-3 cells are a human ovary surface epithelial cell-derived cell line with a highly motile and invasive phenotype. When propagated in culture, these cells exhibit many peripheral actin-rich membrane protrusions. Overexpression of EGFP-LPR1 in SK-OV-3 cells induced a dramatic labeling of membrane protrusions with similar structures to those observed in HeLa and Cos7 cells (data not shown). SK-OV-3 cells were treated with double-stranded synthetic RNAs corresponding to LPR1-specific sequences, RNAi1 and RNAi2, or with a scrambled double-stranded RNA construct (RNAic). When whole cell proteins were analyzed by SDS-PAGE, western blotting and scanning densitometry using the LPR1-selective antibody, we found that RNAi2 produced a marked reduction (~60%) in expression levels of LPR1 in these cells (Fig. 8A). These transfection experiments used pEGFP as a carrier and reporter plasmid that allowed us to identify transfected cells, which were analyzed to quantify the number of filopodia (again defined as actin-rich plasma membrane protrusions <5 μm in length), using the procedure described above for the analysis of filopodia in Cos7 cells. As shown in Fig. 8B and quantified in Fig. 8C, there was an approximate 50% decrease in the number of filopodia in SK-OV-3 cells co-transfected with EGFP and RNAi2 (27.3 filopodia per cell) versus EGFP expressing cells (56.7 filopodia per cell) or cells co-transfected with RNAic and EGFP (57.5 filopodia per cell). These findings suggest that normal expression levels of LPR1 are required for maintenance of filopodia in SK-OV-3 cells.

Discussion

LPR1 is an integral membrane protein that is representative of a class of four proteins with overall homology to the lipid phosphate phosphatases (LPPs). Members of this class of proteins are characterized by variant catalytic domain homology sequences in which residues known to be vital for catalysis in other family members are replaced by non-

conservative substitutions (Sigal et al., 2005). In support of this observation we did not detect lipid phosphatase activity when LPR1 was expressed and assayed using systems that readily support activity of other LPP enzymes. Although in most cases their functions are not known, catalytically inactive variants of a wide variety of enzymes including protein and lipid phosphatases have been described (Kim et al., 2003; Todd et al., 2002). Our results suggest that LPR1 is similarly a 'non-enzyme' relative of the LPPs.

In contrast to its apparent enzymatic inactivity, overexpression of LPR1 induced dramatic morphological changes in multiple cell types. Overexpression of LPR1 resulted in a pronounced labeling of actin rich protrusions in both HeLa and Cos7 cells that, on the basis of their composition and dynamics, were identified as filopodia. Overexpression of LPR1 produced a significant increase in the number of these protrusions. These structures were very dynamic, and were observed retracting and extending from the periphery and the dorsal surface of LPR1-expressing cells. While exogenous expression of a number of actin-binding proteins such as fascin and myosin X has been shown to induce formation of filopodia (Sousa and Cheney, 2005; Svitkina et al., 2003), LPR1, to our knowledge, is a rare example of an integral membrane protein that induces the formation of these structures.

To further characterize filopodia produced by expression of LPR1, we compared the appearance and composition of LPR1-induced filopodia to those provoked by overexpression of activated cdc42. Filopodia induced by overexpression of LPR1 or activated cdc42 both necessarily contain a bundled actin core. Actin is essential for extension of filopodia. Actin polymerization provides the protrusive force that protrudes the plasma membrane allowing for the growth of filopodia. Bundling of actin filaments is necessary to provide the mechanical strength required for an extending filopodium to expand the plasma membrane (Svitkina et al., 2003; Vignjevic et al., 2003). Both actin and the actin-bundling protein fascin were clearly detected along the shaft of filopodia in cells expressing LPR1. Unconventional myosins, specifically myosin X, have been shown to move along the filaments within the extending filopodium and to localize at the filopodial tip (Sousa and Cheney, 2005). Similarly, myosin X was localized to the tips of LPR1-induced filopodia, however its function within these structures remains to be determined.

In contrast to filopodia observed in cells expressing activated cdc42, LPR1-induced filopodia were more persistent, longer, thinner, more motile, and projected from both the cell periphery and dorsal surface. In agreement with our observations that LPR1-induced filopodia differ from filopodia induced by activated cdc42, we found that a dominant-negative allele of cdc42 had no inhibitory effect on the ability of cells expressing LPR1 to form filopodia. This conclusion was further supported by our observations that expression of WASP CRIB domain that sequesters endogenous cdc42 (Nobes and Hall, 1999), also does not interfere with the formation of filopodia in LPR1-expressing cells. Furthermore, expression of an ARP2/3 binding domain of the WASP homolog SCAR, (SCAR WA domain) that sequesters and interferes with the functions of endogenous ARP2/3 complex (Machesky and Insall, 1998), also had no effect on the formation of filopodia in cells overexpressing LPR1. Taken together, these findings

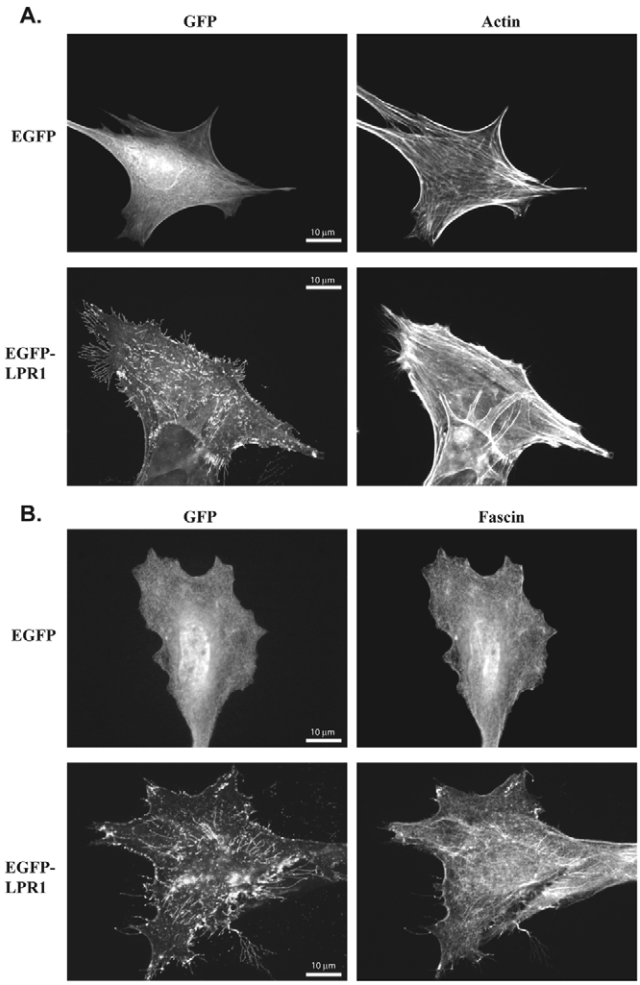

Fig. 7. LPR1 forms filopodia in the absence of Ena/Vasp proteins. MVD7 cells were transfected with vectors for expression of either EGFP or EGFP-LPR1 and visualized by fluorescent microscopy to analyze GFP fluorescence and either actin (A) or fascin (B). Bars, 10 μm.

suggest that the mechanism by which overexpression of LPR1 induces the formation of filopodia is not dependent on the canonical Cdc42-WASP-ARP2/3 pathway of filopodial protrusion.

A recent review article highlighted two distinct types of filopodia with unique morphological appearances (Passey et al., 2004). As reported by many investigators, these authors noted that transient expression of constitutively active alleles of cdc42 resulted in cells having a 'starfish' phenotype, with short and thick filopodia extending predominantly from the cell periphery. By contrast, expression of activated alleles of another small GTPase, Rif, resulted in a cellular phenotype the authors termed 'hedgehog', characterized by the presence of many long, and thin filopodia that most prominently extend from the dorsal surface of the cell. Although more work is clearly needed to compare, characterize and determine the relationship between filopodia characteristic of the starfish and hedgehog phenotypes, our observations suggest that LPR1-induced filopodia are more similar to filopodia induced by activated Rif than those induced by activated cdc42. Focal

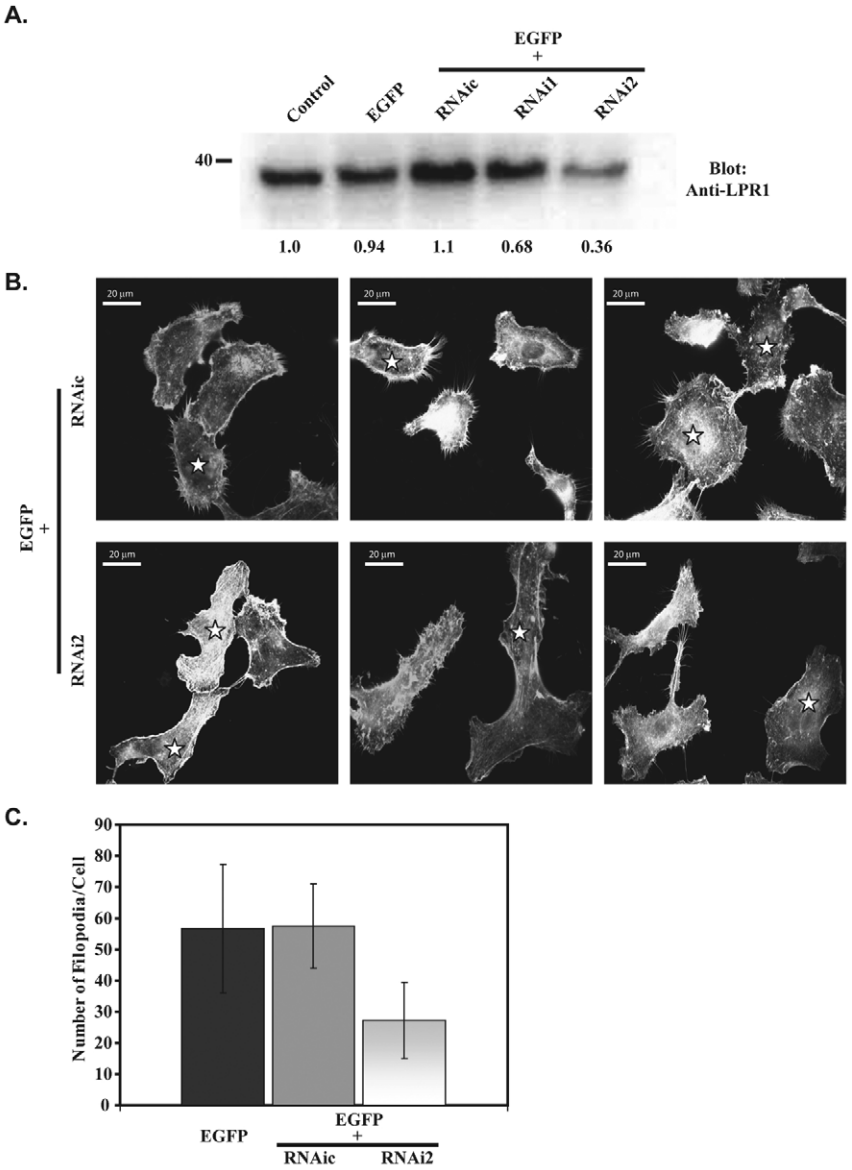

Fig. 8. LPR1 is required for maintenance of membrane protrusions in ovarian epithelial cancer cells. (A) Proteins from SK-OV-3 cells that were either untransfected (control), or transfected with pEGFP alone or in combination with the control double-stranded RNA (RNAic) or two double-stranded siRNAs designed to target LPR1 (RNAi1 and RNAi2) were analyzed by western blotting for LPR1 expression. Immunoreactive species were quantified by scanning densitometry and pixel densities (normalized to control cells) are shown below each lane of the gel. (B) SK-OV-3 cells were co-transfected with pEGFP in combination with either RNAic or RNai2, and actin organization was visualized by fluorescence microscopy. Stars denote cells expressing the EGFP marker. Bars, 20 μm. (C) SK-OV-3 cells were transfected with EGFP alone or in combination with either RNAic or RNAi2. Phalloidin-stained filopodia were counted only in EGFP-expressing cells from the three different categories, and the averages of each were plotted. Error bars denote s.d. The average number of filopodia per cell in EGFP expressing cells was 56.7 (s.d. 20.6, *n*=21). EGFP-expressing cells co-transfected with RNAic had an average of 57.5 filopodia per cell (s.d. 13.5, *n*=26). EGFP expressing cells co-transfected with RNAi2 had an average number of 27.3 filopodia per cell (s.d. 12.3, *n*=25).

adhesion proteins and integrins that are abundant at the tips of cdc42-mediated filopodia (Nobes and Hall, 1995), play a role in attaching these protrusions to the substratum limiting their localization to the periphery of the cell, producing the apparent starfish appearance. These focal adhesion proteins are not found at the tips of Rif-dependent filopodia (Ellis and Mellor, 2000) and we could not detect one such protein, paxillin, at the tips of LPR1-labeled filopodia, although it was readily detected at the base of these structures. The motility of filopodia lacking focal adhesion proteins at their tips is unrestricted by their association with the substratum which, in part, probably results in the hedgehog phenotype characteristic of cells displaying Rif- and LPR1-induced filopodia. Despite the similarities between LPR1- and Rif-induced filpodia, co-expression with dominant-negative Rif did not interfere with the ability of LPR1 to generate filopodia. This finding implies that the induction of filpodia by LPR1 does not involve activation of Rif but does not exclude the possibility that Rif and LPR1 share common effector pathways to regulate the formation of long and thin filopodia at the cellular dorsal and peripheral surfaces.

Our studies also provide some insight into the likely mechanism underlying the induction of filopodia in LPR1-expressing cells. The ‘convergent-elongation’ model of filopodia formation proposes that a filopodium is assembled from the filaments of the dendritic actin network that are bundled together and elongated to form a nascent filopodium (Svitkina et al., 2003; Vignjevic et al., 2003). The length of the filopodium is dependent on the equilibrium between capping proteins that prevent actin polymerization, and anti-capping proteins such as Vasp and Ena that displace capping proteins from the filament tips, allowing for the growth of the filopodium (Bear et al., 2002; Lebrand et al., 2004; Svitkina et al., 2003). Recently published work challenges the ubiquity of this model (Schirenbeck et al., 2006; Snapper et al., 2001; Steffen et al., 2006). Consistent with these new findings, our experiments also suggest that LPR1 induces filopodia by an alternative mechanism. The most intriguing evidence is the ability of LPR1 to generate filopodia in the absence of Vasp or other members of its family, and the lack of these proteins at the tips of LPR1 filopodia. Overexpression of myosin X has

similarly been reported to induce the formation of dorsal filopodia in MV^{D7} cells which, as we have shown is the case for LPR1, must involve a mechanism that is independent of Ena/Vasp proteins (Bohil et al., 2006). Although the authors do not specify the mechanism by which myosin X forms filopodia, these and our results clearly demonstrate that Vasp is not an essential component of all filopodial tip complexes.

The observations raise two major questions about the mechanism by which LPR1 regulates the formation of filopodia: (1) Which protein(s) is responsible for actin nucleation? (2) How are capping proteins prevented from binding to the filopodial tip? One possibility may involve both the nucleating and the anti-capping functions of formins, in particular mDia2 (Higgs, 2005; Nicholson-Dykstra et al., 2005). Because a suitable antibody for visualization of mDia2 or its human ortholog in indirect immunofluorescence studies is not available, we have been unable to determine whether endogenously expressed mDia2 is present at the tips of LPR1-induced filopodia. In preliminary studies using overexpression of tagged variants of mDia2 we observed that that an activated allele, but not the wild-type form of this formin, is localized primarily to the tips of LPR1-labeled filopodia (data not shown). These observations suggest that that LPR1 might influence the localization of activated formins, but does not activate mDia2 directly.

Although the mechanism by which LPR1 regulates the formation of filopodia requires further investigation, mutational studies provide insights into possible mechanisms for regulation of LPR1 and structural determinants within the protein that are important for the induction of filopodia. Firstly, we found that LPR1 mutants in which amino acids known to be important for substrate recognition in enzymatically active LPT family members were replaced with non-conservative substitutions failed to induce the formation of filopodia. These LPR1 mutants displayed a predominantly intracellular localization and failed to induce or localize to filopodia at the plasma membrane. Although we do not know the basis for their altered subcellular localization, these results imply that plasma membrane localization is required for the induction of filopodia by LPR1. Our finding that residues with proven roles in substrate recognition in enzymatically active LPTs are important for LPR1 trafficking and induction of filopodia, suggests that association of LPR1 with an as yet unidentified lipid may regulate these processes. Secondly, we identified a crucial role for the C-terminus of LPR1 in the induction of filopodia. The EGFP-LPR1 C-term Δ43 mutant lacking the C-terminal 43 amino acids localized to the plasma membrane but failed to induce the formation of new peripheral filopodia. This finding suggests a crucial role for the cytoplasmic C-terminus of LPR in the induction of filopodia, and the identification of binding partners that interact with this region of the protein would be a worthwhile strategy for further investigations of the mechanism by which LPR1 induces the formation of filopodia.

To augment our overexpression studies, RNA interference was used to explore the role of endogenously expressed LPR1 in the formation and maintenance of filopodia in SK-OV-3 ovarian cancer cells, which in comparison to other cells and tissues, express the protein at relatively high levels. Expression of LPR1 (as estimated by western blotting of lysates from populations of transiently transfected cells) was suppressed to ~60% of control levels by treatment with an LPR1-selective double-stranded RNA and this was accompanied by a marked decrease in the number of peripheral membrane protrusions. This suggests that, at least in these cells, LPR1 has a role in maintenance of actin-rich structures, such as filopodia. A recent report, however, has shown that overexpression of LPR3, also termed PRG1, promotes neurite extension in cultured neuroblastoma cells (Brauer et al., 2003). LPR3 and the other two members of the LPR family exhibit broad partially overlapping expression patterns (Sigal et al., 2005), so it plausible that the morphological effect of downregulation of LPR1 on this and other cell lines may be limited as a result of functional redundancy between LPR family members.

In conclusion, LPR1 is an integral membrane protein that localizes to the plasma membrane and is heavily enriched along the filopodia. Overexpression of LPR1 promotes the extension of filopodia by a mechanism that is independent of the classic Cdc42-Wasp-Arp2/3 pathway, does not require Ena/Vasp proteins, and does not involve dephosphorylation of lipid monophosphate substrates including LPA and S1P. LPR1 is required for the integrity of actin-rich protrusions in SK-OV-3 ovarian cancer cells. LPR1-induced structures have a characteristic morphology and a distinct protein composition that provide further evidence for its unconventional mechanism of filopodia formation, which differs from the current 'convergent-elongation' model. Further work will be required to elucidate the mechanism by which LPR1 regulates the formation of filopodia.

Materials and Methods

Expression constructs

cDNA constructs containing the complete LPR1 ORF were obtained from Research Genetics or Invitrogen and sequenced using automated procedures (GenBank AY304515). These constructs were used for the generation of recombinant baculovirus vectors using the Fast Bac system (Invitrogen) and for expression of LPR1 in mammalian cells with either C-terminal HA or EGFP-tags using pCDNA (Invitrogen) or pEGFPN1 (Clontech). Site-directed mutants of LPR1 were generated using the QuikChange protocol (Stratagene). Insect and mammalian cell vectors for expression of the LPP enzymes have been described previously (McDermott et al., 2006; Roberts et al., 1998; Sciorra and Morris, 1999). Vectors for expression of wild-type and mutant cdc42 were provided by Channing Der and Keith Burridge, UNC-Chapel Hill. Wild-type and mutant rif constructs were provided by Harry Mellor, Bristol, UK.

Lipid phosphatase assays

Previously described methods for expression and assay of LPPs1-3 were used for investigations of LPR1 (McDermott et al., 2004; Roberts et al., 1998). Assays contained 100 μM substrate and 3.2 mM Triton X-100 or 10 μM substrate complexed with fatty-acid-free BSA at 1 mg/ml. LPP activity was monitored by measuring phosphate release from ^{32}P-labeled substrates.

Antibodies and reagents

The anti-LPR1 antibody was raised in rabbits against a conjugated peptide corresponding to a unique sequence from LPR1, and purified from serum by affinity chromatography using the immobilized peptide. Other primary antibodies used were as follows: Chicken anti-GFP polyclonal (Chemicon International); mouse monoclonal anti-GFP (Covance); mouse monoclonal anti-c-myc antibody (Sigma); mouse monoclonal anti-fascin (DakoCytomation); mouse monoclonal anti-Ha.11 antibody (Covance); purified rabbit polyclonal antibody against paxillin provided by Michael Schaller, UNC-Chapel Hill (Thomas et al., 1999); purified rabbit polyclonal anti-myosin10 antibody provided by Richard Cheney, UNC-Chapel Hill (Berg et al., 2000); polyclonal rabbit anti-vasp, anti-evl and anti-mena antibodies provided by James Bear, UNC-Chapel Hill (Bear et al., 2000). Secondary antibodies used were Alexa Fluor 568 goat anti-rabbit IgG, Alexa Fluor 568 goat anti-mouse IgG, Fluorescein goat anti-mouse IgG all from Molecular Probes, and FITC Donkey anti-chicken IgY (Jackson ImmunoResearch). Horseradish-peroxidase-conjugated secondary antibodies against rabbit and mouse (Chemicon International) were used for western blotting. Rhodamine- and Alexa Fluor 350-conjugated phalloidin (Molecular Probes) were used to visualize actin.

Cell transfections and fluorescence microscopy

HeLa and Cos7 cells were grown on glass coverslips in Dulbecco's modified Eagle's medium (DMEM) containing 10% fetal bovine serum (Gibco), and, where indicated, transfected using lipofectamine. MV^{D7} cells were grown in DMEM supplemented with 15% FBS and transfected using Amaxa nucleoporation protocol for mouse embryonic fibroblasts. Cells were fixed, permeabilized and immunostained using minor modifications of procedures described elsewhere (Sciorra and Morris, 1999). In brief, cells were fixed in 4% paraformaldehyde, permeabilized with 0.1% Triton X-100 in PBS and incubated with Blokhen II blocking reagent (Aves Labs) at a 1:10 dilution in 0.1% Triton X-100 in PBS. Cells were incubated with primary antibodies overnight in PBS at 4°C, washed in PBS and secondary antibodies applied at room temperature for 1 hour. After further washes in PBS, samples were mounted in FluoroSave Reagent (Calbiochem). Images were collected using a Zeiss Axiovert 200 fluorescence microscope with Plan-Neofluar 63× objective and either a Zeiss Axio Cam camera or a Hamamatsu Photonics Orca ER CCD camera. Images were processed using Zeiss Axiovision software or Metamorph software (Universal Imaging) and figures were assembled using Adobe Photoshop and Adobe Illustrator. Confocal images were collected using an Olympus FV500 confocal laser-scanning microscope. A series of images was taken at 0.2-μm intervals through the *z* plane of the cell and were processed to form a projected image.

Live cell imaging

Cells were imaged using an Orca II CCD camera (Hamamatsu) with Metamorph software (Universal Imaging) to control illumination shutters and camera exposure. Timelapse images were obtained by sequential epifluorescent and phase illumination with a 63× phase 3 lens (Zeiss, Thornwood, NJ). Time-lapse intervals were 5 seconds and exposure times were 100-300 milliseconds, depending on the time-lapse interval and level of fluorescence. Cells were imaged over periods of 0-60 minutes in HEPES-buffered Opti-MEM with 5% serum at 37°C. The images were edited and movies generated using ImageJ software (Wayne Rasband, NIMH) and converted to Quicktime files using Quicktime Pro. Three-dimensional confocal microscopy was performed using an Olympus FV500 confocal laser-scanning microscope in HEPES-buffered Opti-Mem with 5% serum at 37°C. A series of images was taken at a single time point at 0.2-μm intervals through the *z* plane of the cell and were processed to form a projected image.

RNA interference

We used minor adaptations of a previously published procedure (McManus and Sharp, 2002). In brief, SK-OV-3 cells were plated in six-well plates at 2.5×10^5 cells/well in McCoy's media supplemented with 10% FBS and allowed to grow overnight. Cells were transfected with 1 μg RNA and 1 μg pEGFP in 1 ml of serum free McCoy's media. After 4 hours, a further 1 ml of McCoy's media supplemented with 20% FBS was added to each well. Cells were allowed to grow for 48 hours at 37°C before they were processed for fluorescence microscopy or western blot analysis. RNAs were from Dharmacon (Lafayette, CO) and RNA duplexes were prepared according to the manufacturer's instructions. The RNA sequences used were (sense strands) RNAi 1, CAC UCA ACG AAG UUA UUC C; RNAi 2, CUU CGA AGG AUC AUA AGA U; RNAic, ACU CUA UCU GCA CGC UGA C.

Western blot analysis

Protein concentration was determined by BCA protein assay (Pierce) using BSA as a standard. Samples were separated by 12.5% SDS-PAGE or 4-10% gradient SDS-PAGE, and the proteins were transferred to a PVDF membrane (Amersham Biosciences). The membrane was incubated with primary antibody, followed by horseradish-peroxidase-conjugated secondary antibody. The immunoreactive bands were detected with SuperSignal West Pico chemiluminescent substrate (Pierce).

Other procedures

Calculations of number of filopodia in Cos7 and SK-OV-3 cells were done as discussed in the legend to Fig. 2. Calculations of LPR1-induced filopodia in the presence of DN Rif and Cdc42 mutants were performed as discussed in Fig. 5. Plots were constructed using Excel. In cases where representative data are shown experiments have been repeated a minimum of three times with comparable results.

This work was supported by NIH grants DC03299 to R.E.C., GM00678 to O.A.Q. and GM54388 and CA096496 to A.J.M. Y.J.S. is an American Heart Association predoctoral fellow. O.A.Q. was also supported by SPIRE postdoctoral training grant at UNC. We are grateful to Michael Shaller, Keith Burridge, Channing Der, Ken Jacobson, James Bear, Carol Otey, and members of their laboratories for reagents, advice and assistance with aspects of this work. We thank Frank Gertler for MV^{D7} cells. Finally we acknowledge the important contributions of Vicki Sciorra to this research.

References

Atilgan, E., Wirtz, D. and Sun, S. X. (2006). Mechanics and dynamics of actin-driven thin membrane protrusions. *Biophys. J.* **90**, 65-76.

Bear, J. E., Loureiro, J. J., Libova, I., Fassler, R., Wehland, J. and Gertler, F. B. (2000). Negative regulation of fibroblast motility by Ena/VASP proteins. *Cell* **101**, 717-728.

Bear, J. E., Svitkina, T. M., Krause, M., Schafer, D. A., Loureiro, J. J., Strasser, G. A., Maly, I. V., Chaga, O. Y., Cooper, J. A., Borisy, G. G. et al. (2002). Antagonism between Ena/VASP proteins and actin filament capping regulates fibroblast motility. *Cell* **109**, 509-521.

Berg, J. S., Derfler, B. H., Pennisi, C. M., Corey, D. P. and Cheney, R. E. (2000). Myosin-X, a novel myosin with pleckstrin homology domains, associates with regions of dynamic actin. *J. Cell Sci.* **113**, 3439-3451.

Bishop, A. L. and Hall, A. (2000). Rho GTPases and their effector proteins. *Biochem. J.* **348**, 241-255.

Bohil, A. B., Robertson, B. W. and Cheney, R. E. (2006). Myosin-X is a molecular motor that functions in filopodia formation. *Proc. Natl. Acad. Sci. USA* **103**, 12411-12416.

Brauer, A. U., Savaskan, N. E., Kuhn, H., Prehn, S., Ninnemann, O. and Nitsch, R. (2003). A new phospholipid phosphatase, PRG-1, is involved in axon growth and regenerative sprouting. *Nat. Neurosci.* **6**, 572-578.

Brindley, D. N. and Waggoner, D. W. (1998). Mammalian lipid phosphate phosphohydrolases. *J. Biol. Chem.* **273**, 24281-24284.

Czuchra, A., Wu, X., Meyer, H., van Hengel, J., Schroeder, T., Geffers, R., Rottner, K. and Brakebusch, C. (2005). Cdc42 is not essential for filopodium formation, directed migration, cell polarization, and mitosis in fibroblastoid cells. *Mol. Biol. Cell* **16**, 4473-4484.

Ellis, S. and Mellor, H. (2000). The novel Rho-family GTPase rif regulates coordinated actin-based membrane rearrangements. *Curr. Biol.* **10**, 1387-1390.

Etienne-Manneville, S. and Hall, A. (2002). Rho GTPases in cell biology. *Nature* **420**, 629-635.

Evangelista, M., Zigmond, S. and Boone, C. (2003). Formins: signaling effectors for assembly and polarization of actin filaments. *J. Cell Sci.* **116**, 2603-2611.

Faix, J. and Rottner, K. (2006). The making of filopodia. *Curr. Opin. Cell Biol.* **18**, 18-25.

Higgs, H. N. (2005). Formin proteins: a domain-based approach. *Trends Biochem. Sci.* **30**, 342-353.

Holt, M. R., Critchley, D. R. and Brindle, N. P. (1998). The focal adhesion phosphoprotein, VASP. *Int. J. Biochem. Cell Biol.* **30**, 307-311.

Kalil, K. and Dent, E. W. (2005). Touch and go: guidance cues signal to the growth cone cytoskeleton. *Curr. Opin. Neurobiol.* **15**, 521-526.

Kim, S. A., Vacratsis, P. O., Firestein, R., Cleary, M. L. and Dixon, J. E. (2003). Regulation of myotubularin-related (MTMR)2 phosphatidylinositol phosphatase by MTMR5, a catalytically inactive phosphatase. *Proc. Natl. Acad. Sci. USA* **100**, 4492-4497.

Krugmann, S., Jordens, I., Gevaert, K., Driessens, M., Vandekerckhove, J. and Hall, A. (2001). Cdc42 induces filopodia by promoting the formation of an IRSp53:Mena complex. *Curr. Biol.* **11**, 1645-1655.

Lebrand, C., Dent, E. W., Strasser, G. A., Lanier, L. M., Krause, M., Svitkina, T. M., Borisy, G. G. and Gertler, F. B. (2004). Critical role of Ena/VASP proteins for filopodia formation in neurons and in function downstream of netrin-1. *Neuron* **42**, 37-49.

Machesky, L. M. and Insall, R. H. (1998). Scar1 and the related Wiskott–Aldrich syndrome protein, WASP, regulate the actin cytoskeleton through the Arp2/3 complex. *Curr. Biol.* **8**, 1347-1356.

McDermott, M. I., Sigal, Y. J., Sciorra, V. A. and Morris, A. J. (2004). Is PRG-1 a new lipid phosphatase? *Nat. Neurosci.* **7**, 789; author reply 789-790.

McDermott, M. I., Sigal, Y. J., Crump, J. S. and Morris, A. J. (2006). Enzymatic analysis of lipid phosphate phosphatases. *Methods* **39**, 169-179.

McManus, M. T. and Sharp, P. A. (2002). Gene silencing in mammals by small interfering RNAs. *Nat. Rev. Genet.* **3**, 737-747.

Nicholson-Dykstra, S., Higgs, H. N. and Harris, E. S. (2005). Actin dynamics: growth from dendritic branches. *Curr. Biol.* **15**, R346-R357.

Nobes, C. D. and Hall, A. (1995). Rho, rac, and cdc42 GTPases regulate the assembly of multimolecular focal complexes associated with actin stress fibers, lamellipodia, and filopodia. *Cell* **81**, 53-62.

Nobes, C. D. and Hall, A. (1999). Rho GTPases control polarity, protrusion, and adhesion during cell movement. *J. Cell Biol.* **144**, 1235-1244.

Passey, S., Pellegrin, S. and Mellor, H. (2004). What is in a filopodium? Starfish versus hedgehogs. *Biochem. Soc. Trans.* **32**, 1115-1117.

Pellegrin, S. and Mellor, H. (2005). The Rho family GTPase Rif induces filopodia through mDia2. *Curr. Biol.* **15**, 129-133.

Peng, J., Wallar, B. J., Flanders, A., Swiatek, P. J. and Alberts, A. S. (2003). Disruption of the Diaphanous-related formin Drf1 gene encoding mDia1 reveals a role for Drf3 as an effector for Cdc42. *Curr. Biol.* **13**, 534-545.

Perez-Moreno, M., Jamora, C. and Fuchs, E. (2003). Orchestrating cellular signals at adherens junctions. *Cell* **112**, 535-548.

Roberts, R., Sciorra, V. A. and Morris, A. J. (1998). Human type 2 phosphatidic acid phosphohydrolases. Substrate specificity of the type 2a, 2b, and 2c enzymes and cell surface activity of the 2a isoform. *J. Biol. Chem.* **273**, 22059-22067.

Samarin, S., Romero, S., Kocks, C., Didry, D., Pantaloni, D. and Carlier, M. F. (2003). How VASP enhances actin-based motility. *J. Cell Biol.* **163**, 131-142.

Savaskan, N. E., Brauer, A. U. and Nitsch, R. (2004). Molecular cloning and expression

regulation of PRG-3, a new member of the plasticity-related gene family. *Eur. J. Neurosci.* **19**, 212-220.

Schirenbeck, A., Bretschneider, T., Arasada, R., Schleicher, M. and Faix, J. (2005). The Diaphanous-related formin dDia2 is required for the formation and maintenance of filopodia. *Nat. Cell Biol.* **7**, 619-625.

Schirenbeck, A., Arasada, R., Bretschneider, T., Stradal, T. E., Schleicher, M. and Faix, J. (2006). The bundling activity of vasodilator-stimulated phosphoprotein is required for filopodium formation. *Proc. Natl. Acad. Sci. USA* **103**, 7694-7699.

Sciorra, V. A. and Morris, A. J. (1999). Sequential actions of phospholipase D and phosphatidic acid phosphohydrolase 2b generate diglyceride in mammalian cells. *Mol. Biol. Cell* **10**, 3863-3876.

Sigal, Y. J., McDermott, M. I. and Morris, A. J. (2005). Integral membrane lipid phosphatases/phosphotransferases: common structure and diverse functions. *Biochem. J.* **387**, 281-293.

Snapper, S. B., Takeshima, F., Anton, I., Liu, C. H., Thomas, S. M., Nguyen, D., Dudley, D., Fraser, H., Purich, D., Lopez-Ilasaca, M. et al. (2001). N-WASP deficiency reveals distinct pathways for cell surface projections and microbial actin-based motility. *Nat. Cell Biol.* **3**, 897-904.

Sousa, A. D. and Cheney, R. E. (2005). Myosin-X: a molecular motor at the cell's fingertips. *Trends Cell Biol.* **15**, 533-539.

Starz-Gaiano, M., Cho, N. K., Forbes, A. and Lehmann, R. (2001). Spatially restricted activity of a Drosophila lipid phosphatase guides migrating germ cells. *Development* **128**, 983-991.

Steffen, A., Faix, J., Resch, G. P., Linkner, J., Wehland, J., Small, J. V., Rottner, K. and Stradal, T. E. (2006). Filopodia formation in the absence of functional WAVE and Arp2/3 complexes. *Mol. Biol. Cell* **17**, 2581-2591.

Svitkina, T. M. and Borisy, G. G. (1999). Arp2/3 complex and actin depolymerizing factor/cofilin in dendritic organization and treadmilling of actin filament array in lamellipodia. *J. Cell Biol.* **145**, 1009-1026.

Svitkina, T. M., Bulanova, E. A., Chaga, O. Y., Vignjevic, D. M., Kojima, S., Vasiliev, J. M. and Borisy, G. G. (2003). Mechanism of filopodia initiation by reorganization of a dendritic network. *J. Cell Biol.* **160**, 409-421.

Thomas, J. W., Cooley, M. A., Broome, J. M., Salgia, R., Griffin, J. D., Lombardo, C. R. and Schaller, M. D. (1999). The role of focal adhesion kinase binding in the regulation of tyrosine phosphorylation of paxillin. *J. Biol. Chem.* **274**, 36684-36692.

Todd, A. E., Orengo, C. A. and Thornton, J. M. (2002). Sequence and structural differences between enzyme and nonenzyme homologs. *Structure* **10**, 1435-1451.

Tokuo, H. and Ikebe, M. (2004). Myosin X transports Mena/VASP to the tip of filopodia. *Biochem. Biophys. Res. Commun.* **319**, 214-220.

Vignjevic, D., Yarar, D., Welch, M. D., Peloquin, J., Svitkina, T. and Borisy, G. G. (2003). Formation of filopodia-like bundles in vitro from a dendritic network. *J. Cell Biol.* **160**, 951-962.

Welch, M. D. and Mullins, R. D. (2002). Cellular control of actin nucleation. *Annu. Rev. Cell Dev. Biol.* **18**, 247-288.

Wood, W. and Martin, P. (2002). Structures in focus—filopodia. *Int. J. Biochem. Cell Biol.* **34**, 726-730.

Yang, F., Moss, L. G. and Phillips, G. N., Jr (1996). The molecular structure of green fluorescent protein. *Nat. Biotechnol.* **14**, 1246-1251.

Zhang, H., Berg, J. S., Li, Z., Wang, Y., Lang, P., Sousa, A. D., Bhaskar, A., Cheney, R. E. and Stromblad, S. (2004). Myosin-X provides a motor-based link between integrins and the cytoskeleton. *Nat. Cell Biol.* **6**, 523-531.